

doi: 10.17586/2226-1494-2023-23-6-1136-1142

Raman spectroscopy of nanocomposites ZnO/ZnS and ZnO/ZnSe obtained by solvothermal-microwave synthesis method

Yolanda Rati¹, Ari Sulistyo Rini², Ali Umar Akrajas³, Miranti Agustin⁴

¹ Institut Teknologi Bandung, Bandung, 40132, Indonesia

^{2,4} Universitas Riau, Pekanbaru, 28293, Indonesia

³ Universiti Kebangsaan Malaysia, Selangor, 43600, Malaysia

¹ yolandarati@gmail.com, <https://orcid.org/0000-0003-0222-6014>

² ari.sulistyo@lecturer.unri.ac.id, <https://orcid.org/0000-0002-5435-2568>

³ akrajas@ukm.edu.my, <https://orcid.org/0000-0001-8299-4827>

⁴ mirantiagustin17@gmail.com, <https://orcid.org/0009-0007-1358-0496>

Abstract

We report the ZnO/ZnS and ZnO/ZnSe nanocomposites synthesized using the solvothermal-microwave method. Raman analysis was thoroughly studied to explain phonon vibration mode in this paper. The strong intensity confirms the high-frequency phonon mode of hexagonal wurtzite ZnO. Also, the presence of Raman intensity of the cubic ZnS and ZnSe structures indicates the longitudinal optical phonon mode. In addition, we find several slight shifts in all ZnO modes for ZnO/ZnS and ZnO/ZnSe which demonstrate stress and strain in the crystal lattice. We investigate the change in particle size from confocal Raman microscopy. Therefore, the modifications to the material structure and particle size have enhanced its characteristics. Accordingly, the nanocomposite heterostructures by the simple chemical method are attractive materials suitable for optoelectronic devices.

Keywords

heterostructures, phonon vibration mode, Raman, solvothermal-microwave, wurtzite

For citation: Rati Y., Rini A.S., Akrajas A.U., Agustin M. Raman spectroscopy of nanocomposites ZnO/ZnS and ZnO/ZnSe obtained by solvothermal-microwave synthesis method. *Scientific and Technical Journal of Information Technologies, Mechanics and Optics*, 2023, vol. 23, no. 6, pp. 1136–1142. doi: 10.17586/2226-1494-2023-23-6-1136-1142

УДК 544.02

Рамановская спектроскопия нанокомпозитов ZnO/ZnS и ZnO/ZnSe,

полученных методом сольвотермического микроволнового синтеза

Иоланда Рати¹, Ари Сулисто Рини², Али Умар Акраджас³, Миранті Агустін⁴

¹ Бандунгский технологический институт, Бандунг, 40132, Индонезия

^{2,4} Университет Риау, Пеканбару, 28293, Индонезия

³ Национальный университет Малайзии, Селангор, 43600, Малайзия

¹ yolandarati@gmail.com, <https://orcid.org/0000-0003-0222-6014>

² ari.sulistyo@lecturer.unri.ac.id, <https://orcid.org/0000-0002-5435-2568>

³ akrajas@ukm.edu.my, <https://orcid.org/0000-0001-8299-4827>

⁴ mirantiagustin17@gmail.com, <https://orcid.org/0009-0007-1358-0496>

Аннотация

Представлены нанокомпозиты ZnO/ZnS и ZnO/ZnSe, синтезированные сольвотермо-микроволновым методом. Для объяснения режима фононных колебаний применен метод рамановской спектроскопии. Полученная высокая интенсивность рамановского рассеяния подтвердила высокочастотную фононную моду гексагонального вюрцита ZnO. Наличие интенсивного комбинационного рассеяния света кубических структур ZnS и ZnSe свидетельствует о существовании продольной оптической фононной моды. Обнаружены небольшие сдвиги во всех модах ZnO для ZnO/ZnS и ZnO/ZnSe, которые указывают на наличие напряжения и деформации в кристаллической решетке.

© Rati Y., Rini A.S., Akrajas A.U., Agustin M., 2023

Исследованы изменения размера частиц с помощью конфокальной рамановской микроскопии. Показано, что изменения структуры и размеров частиц материала улучшили его характеристики. Подтверждено, что нанокомпозитные гетероструктуры, полученные простым химическим методом, применимы для создания оптоэлектронных устройств.

Ключевые слова

гетероструктуры, фононная мода колебаний, комбинационное рассеяние света, сольвотермо-микроволновый синтез, вюрцит

Ссылка для цитирования: Рати И., Рини А.С., Акраджас А.У., Агустин М. Рамановская спектроскопия нанокомпозитов ZnO/ZnS и ZnO/ZnSe, полученных методом сольвотермического микроволнового синтеза // Научно-технический вестник информационных технологий, механики и оптики. 2023. Т. 23, № 6. С. 1136–1142 (на англ. яз.). doi: 10.17586/2226-1494-2023-23-6-1136-1142

Introduction

Zinc oxide (ZnO) is a widely researched semiconductor material due to its outstanding electronic, optical, and structural features. It recently also gets more attention in several applications, especially in the electronics industry. At room temperature, ZnO in a hexagonal wurtzite structure (for hexagonal structure, lattice parameters a , b , and c are the lengths between two points on the corners of a unit cell: $a = b = 0.3296$ nm and $c = 0.5206$ nm) has a wide band gap energy (direct) of 3.37 eV and a large exciton binding energy of 60 meV [1]. ZnO is a versatile material due to its high chemical and thermal durability, enormous surface area, excellent photoelectric, UV-sensitive, and good compatibility [2]. So, it is used for optoelectronic devices such as sensors [3], light-emitting diodes [4], and photocatalysts [5].

Covering ZnO with other semiconductors in the form of core-shell structure can enhance its structural and optical properties. Moreover, it can upgrade ZnO performance for broader applications. Zinc sulfide (ZnS) is a semiconducting material with a broad energy band gap of 3.80 eV in hexagonal wurtzite and 3.68 eV in cubic zinc blende phase [6]. The large absorption spectrum makes it a suitable candidate for sensors and electroluminescence devices [7]. On the other hand, the zinc selenide (ZnSe) semiconductor has a lower band gap energy of 2.86–2.94 eV than the ZnO [8]. ZnSe also has higher conductivity than ZnO and is sensitive in a wide visible spectrum, so it is commonly applied for optoelectronic and photoelectric devices [9].

A nanocomposite is a mixture of two or several materials at a nanometer size scale. Baranowska et al. [10] reported that coating ZnO with ZnS (ZnO/ZnS) nanocomposites has enhanced its environmental stability and improved the electrical properties of ZnO thin films. Khan et al. [11] synthesized ZnO/ZnS hybrid by wet chemical method and found that the composites produced a synergistic effect to decompose dye efficiency in photocatalytic application due to reduced charge recombination and a rise in intrinsic oxygen vacancies. Incorporating the ZnS layer on ZnO/perovskite also demonstrates rapid electron transfer and reduces the interfacial recombination, hence enhancing the solar cell performance. It also attributed to sulfide which has strong surface interaction with Pb²⁺ resulting in novel electron transport route [12]. Visible light photocatalysis of porous ZnO/ZnSe that was prepared by microwave-assisted hydrothermal method recorded a high activity properties [13]. Kamruzzaman and Zapien [14] reported

that core-shell ZnO/ZnSe nanowires realized high-performance solar cells. It is due to high absorption with a low band gap (1.90 eV) as well as reducing surface defects that marked by decreased Raman intensity of ZnO. All of this performance depends on the optical properties of the material. One of them is studied on interactions in crystal lattice vibrations related to optical vibration modes.

In this paper, we report the solvothermal-microwave synthesis of ZnO/ZnS and ZnO/ZnSe nanocomposites and investigate their optical and structural characteristic by the Raman spectroscopy analysis. The microwave-solvothermal method has been widely reported as an effective method for semiconducting oxide nanostructures synthesis [15]. This approach has low energy consumption, fast reaction, good quality crystal product, and simple method. We carried out a Raman analysis to study the structural properties of the nanocomposites of ZnO/ZnS and ZnO/ZnSe synthesized by this route. Raman spectroscopy is one of the most versatile techniques for material characterization. It provides information on the crystal lattice structure and defects that can be known through the optical vibration mode of Raman spectra. We identified the cubic phase of ZnS and ZnSe on the Raman spectrum of ZnO/ZnS and ZnO/ZnSe. Additionally, a slight shift of the wurtzite ZnO optical mode indicates the stress and strain effects of the crystal lattice, which reveals that structural alteration has occurred due to the coating process.

Materials and methods

Materials

The Flourine Tin Oxide (FTO) substrates (purchased from the Kaivo instrument, China) were used throughout this work. Analytical reagents, including zinc acetate dihydrate ($\text{Zn}(\text{CH}_3\text{COO})_2 \cdot 2\text{H}_2\text{O}$), zinc nitrate hexahydrate ($\text{Zn}(\text{NO}_3)_2 \cdot 6\text{H}_2\text{O}$), and hexamethylenetetramine ($\text{C}_6\text{H}_{12}\text{N}_4$) were purchased from Sigma Aldrich, USA. Other chemicals, such as sodium sulfide (Na_2S), sulfur (S), selenium (Se), sodium borohydride (NaBH_4), and 99 % ethanol ($\text{C}_2\text{H}_5\text{OH}$) were acquired from R&M Chemicals, Malaysia. Deionized (DI) water originated from the Mili-Q water purification system (approximately 18.2 MΩ).

Synthesis of pristine ZnO

First, 10 mM of $\text{Zn}(\text{CH}_3\text{COO})_2 \cdot 2\text{H}_2\text{O}$ was diluted in ethanol as seed solution. ZnO seeds are prepared via spin coating seed solution at 3000 rpm and thermal annealing (300 °C) processes on the FTO substrate. Furthermore, pristine ZnO was grown on ZnO seeds by the solvothermal method. 100 mM aqueous solution of $\text{Zn}(\text{NO}_3)_2 \cdot 6\text{H}_2\text{O}$

and $C_6H_{12}N_4$ (equimolar) was reacted in vial. Then, it was heated at $90^\circ C$ for 3 h. The sample obtained was cleaned from residual molecules using DI water.

Route of nanocomposites ZnO/ZnS and ZnO/ZnSe

The synthesis of ZnO/ZnS and ZnO/ZnSe nanocomposites ZnO/ZnS and ZnO/ZnSe were carried out by microwave heating. Pristine ZnO was immersed in growth solution and reacted with 2 ml of Na_2S , $NaBH_4 + S$, and $NaBH_4 + Se$ (equimolar) in different vials. $NaBH_4$ acts as a reducing agent to S or Se solution. The three samples were named ZnO/ Na_2S , ZnO/NBS, and ZnO/NBSe. Each sample was irradiated at power 360 W for 20 s using a microwave oven. Finally, the nanocomposite samples were rinsed in DI water, flushed with nitrogen, and annealed at $300^\circ C$ for 1 h using a tube furnace.

Characterization

Raman spectra were performed at ambient condition using a Confocal Raman Microscopy (CRM 200 WiTec) with charged-coupled device (CCD) camera. An excitation source of 532 nm (Argon ion laser) and power 10 mW were used for recording the spectra. The limit spectral range used was $150\text{--}650\text{ cm}^{-1}$ with a typical resolution of 1.9 cm^{-1} and was focused into a spot size of about $10\text{ }\mu\text{m}$ diameter.

Results and discussion

Raman spectrum at room temperature conditions of ZnO nanocomposites in the range of $150\text{--}650\text{ cm}^{-1}$ is shown in Fig. 1. Raman spectroscopy is an effective way to study crystal structure, lattice and defect of films surface by analyzing the phonon frequency of the Raman peak. Raman peaks of pristine ZnO by solvothermal route appear at the frequencies 333, 382, 417–424, 438, and 574 cm^{-1} , which are assigned as $E_2^{\text{High}} - E_2^{\text{Low}}$, $A_1(\text{TO})$, $E_1(\text{TO})$, E_2^H , and $E_1(\text{LO})$ modes, respectively. It is a characteristic of the fundamental optical mode (Γ_{opt}) from the Brillouin zone consisting of the longitudinal optic (LO) and transverse optic (TO) of ZnO with C_{6v} (P_63mc) point group symmetry [16].

The strong peak E_2^H (high-frequency phonons) at 438 cm^{-1} demonstrates the fingerprint of the hexagonal wurtzite structure ZnO with good crystallinity [17]. The vibration of the heavy Zn sublattice and oxygen vibration are linked with this non polar mode [18]. It has a relatively higher intensity compared to others. Raman peak of pristine ZnO is narrow and sharp. ZnO/ Na_2S displays a wide and slightly shifted peak (4 cm^{-1}) at 434 cm^{-1} . It is due to the relaxation stress (internal strain) of the intermolecular [19]. Raman peak frequencies of ZnO/NBS and ZnO/NBSe are similar to pristine ZnO. However, the intensity is very low in ZnO/NBSe. It is assumed that the ZnO structure of the nanocomposite ZnO/ZnSe has changed.

The second-order Raman spectrum detected at 333 cm^{-1} in pristine ZnO is attributed to the phonon boundary zone $E_2^H - E_2^L$, which is associated with multiphonon scattering nonpolar mode [20]. Frequency shifts in ZnO/ Na_2S and ZnO/NBS have occurred at 331 cm^{-1} and 330 cm^{-1} , respectively. Raman peak of ZnO/NBSe remains constant, although the intensity is barely apparent. The broad hump between $560\text{--}610\text{ cm}^{-1}$ exhibits the lattice vibrations $E_1(\text{LO})$ mode within the pristine ZnO with a peak at

574 cm^{-1} . $E_1(\text{LO})$ mode refers to the characteristic of randomly ZnO crystallite orientation on the substrate [21]. It occurs due to intrinsic defects, such as oxygen vacancies, interstitial Zn, and the resonance effect in the ZnO crystal lattice at the excitation wavelength [22]. A slight shift occurs at 572 cm^{-1} and 571 cm^{-1} for ZnO/ Na_2S and ZnO/NBS, respectively. This vibration mode was not found in ZnO/NBSe because of the broadening effect of this peak.

The $E_1(\text{TO})$ mode from pristine ZnO is detected at 417 cm^{-1} and 424 cm^{-1} . On ZnO nanocomposites, this Raman peak is not clearly seen. A small shift (3 cm^{-1}) occurs in ZnO/NBS at 414 cm^{-1} and 421 cm^{-1} . Furthermore, the lowest intensity is found at 382 cm^{-1} which represents $A_1(\text{TO})$ mode. The $A_1(\text{TO})$ mode of ZnO/NBS and ZnO/NBSe shift toward a higher frequency at 385 cm^{-1} and 393 cm^{-1} . This indicates to compressive stress effect of the crystal lattice of heterostructural materials. Moreover, it is due to interlayer attracting forces being decreased [15]. On the other hand, the Raman peak is not as apparent in the nanocomposite ZnS as well as ZnSe. It is probably due to a change in the structure of the nanocomposite there by weakening the intensity of this mode. E_1 and A_1 are polar of Raman and infrared active because have LO and TO Raman frequency [20].

Additional mode at 343 cm^{-1} in ZnO/ Na_2S and 342 cm^{-1} in ZnO/NBS using solvothermal-microwave synthesis is related to ZnS indicating $T_2(\text{LO})$ optical mode. It is attributed to the first-order Raman frequency characteristic of zinc blende (β -ZnS cubic) [10]. ZnS has $F43m$ (T_d^2) space group with a high frequency of single LO phonon [23]. TO phonon (277 cm^{-1}) not observed in

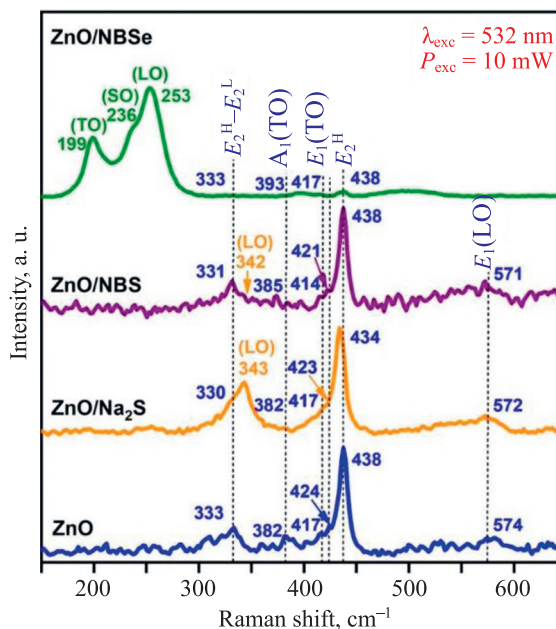


Fig. 1. Raman scattering spectrum of ZnO, ZnO/ Na_2S , ZnO/NBS, and ZnO/NBSe by solvothermal-microwave synthesis. The wavelength of the excitation source is 532 nm, and the power is 10 mW. The major peak is attributed to E_2^H at 438 cm^{-1} from hexagonal wurtzite ZnO. A slightly shifted of ZnO Raman peaks (blue text) is found for nanocomposite samples. The ZnS (orange graph) and ZnSe (green graph) peaks exhibit at 343 cm^{-1} and 253 cm^{-1}

the Raman spectrum. The cubic structure revealed the low-temperature phase, while hexagonal ZnS represented the high-temperature phase. In a solid-liquid chemical process, ZnO and Na₂S were reported to create ZnS cubic with good crystalline properties [24], which is seen from the high peak of Raman frequency. So, the wurtzite structure of ZnO has changed due to the presence of the zinc blende structure of ZnS. On the other hand, ZnO/NBS reveals the low intensity of the Raman peak of ZnS. It is due to NaBH₄ does not optimally reduce sulfur powder. At ambient temperature, sulfur is largely inert to sodium borohydride. To be well reduced and have good dispersion, the molar ratio of NaBH₄ to sulfur is used 15:1 [25]. Overall, the presence of a ZnS confirms that the nanocomposite heterostructure grown on ZnO was successfully synthesized. But, the structure of ZnO/ZnS is still dominated by hexagonal wurtzite because the major peak is found in the E_2^H mode of ZnO.

Raman spectra of ZnSe synthesized using the microwave method are revealed at 199, 236, and 253 cm⁻¹. The peak at 253 cm⁻¹ is assigned to the first-order LO phonon mode of zinc blende ZnSe crystal [26]. The appearance of the LO phonon demonstrates a good crystalline structure. An interesting strong peak of ZnSe along with the low intensity of E_2^H mode ZnO indicates a transformed structure. A similar condition has been reported by ZnO/ZnSe nanowires [14]. In a neutral solution, the reduction of Se by NaBH₄ provides distinct outcomes compared to S. It is reported that can reduce Se more effectively than sulfur [27]. The TO phonon mode of ZnSe is observed at 199 cm⁻¹. Se effect presence is

associated with a low strain in this mode [9]. Furthermore, SO (surface optic) scattering which appears between LO and TO frequency is assigned at 236 cm⁻¹. It represents the feature of small-size nanostructures [28]. Accordingly, in this work, ZnO/ZnSe heterostructure has been confirmed completely.

Fig. 2 exhibits the surface morphology of ZnO nanocomposites using solvothermal-microwave synthesis at a scale bar of 10 μm using CCD camera integrated with confocal Raman microscopy. The red box on this figure reveals the spot area of the laser source (Ar ion, $\lambda = 532$ nm). Pristine ZnO (Fig. 2, a) shows a uniform nanorod shape and is clearly seen. The nanorod size slightly increased in ZnO/Na₂S (Fig. 2, b). Whereas in ZnO/NBS (Fig. 2, c), the diameter nanorods are increasing. Furthermore, the nanorods changed shape and decreased in size in ZnO/NBSe (Fig. 2, d). Also, it appears orange with large red-brown grains. It occurs because of NaBH₄ and Se reacted in water to form a brownish-red solution. While the reduction of NaBH₄ on S produces a white or slightly yellow solution. It is not so obvious in ZnO/NBS image. The surface morphology was more detail observed using field emission scanning electron microscope analysis.

Overall, Raman spectra detected the existence of phonon vibration modes for all samples. The vibrational modes for ZnO, ZnS, and ZnSe observed confirm the formation of ZnO/ZnS and ZnO/ZnSe nanocomposites by the solvothermal-microwave method. The heterostructures materials from polar semiconductor combination ZnO/ZnS and ZnO/ZnSe can be potentially applied to the optoelectronic device.

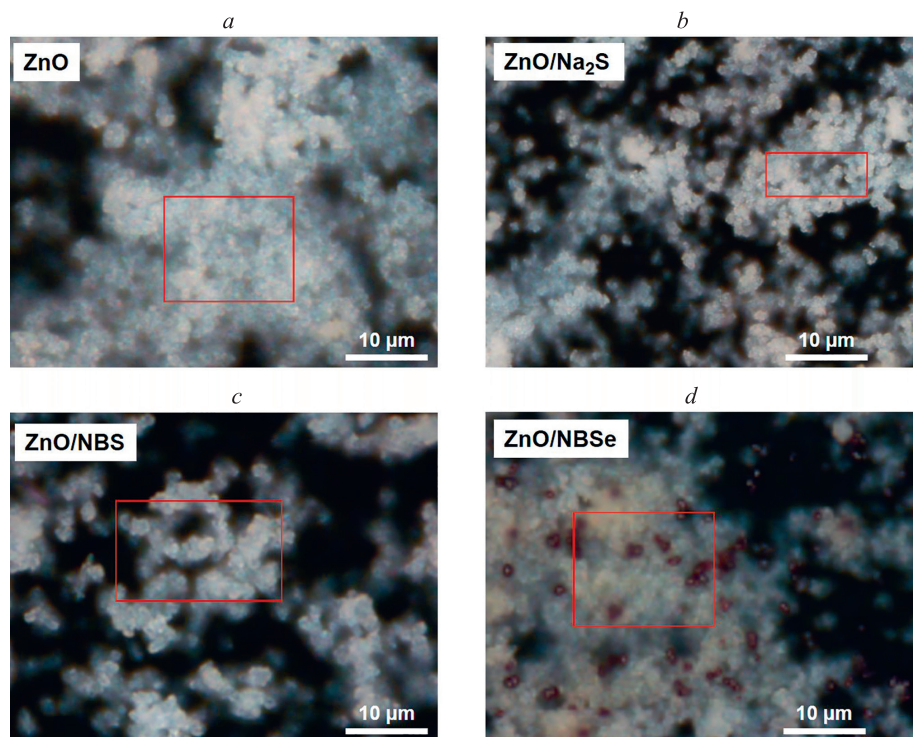


Fig. 2. Images recorded by CCD camera of confocal Raman microscopy in spot size 10 μm of ZnO nanocomposites (the red box is spot laser area using Ar ion with wavelength source at 532 nm). Pristine ZnO shows clustered forms of nanorods (a). Next, ZnO/Na₂S (b) and ZnO/NBS (c) exhibit size gradually increase in the nanorod. In ZnO/NBSe (d), it saw orange small nanorods and brownish-red grains

Conclusion

Synthesis of nanocomposites ZnO/ZnS and ZnO/ZnSe has been successfully carried out by the solvothermal-microwave method. Raman analysis demonstrates hexagonal wurtzite ZnO mode from the major peak at 438 cm^{-1} which identifies the E_2^{H} phonon. Other peaks of ZnO were found at 333, 382, 417–424, and 574 cm^{-1} attributed $E_2^{\text{H}}\text{--}E_2^{\text{L}}$, $A_1(\text{TO})$, $E_1(\text{TO})$, and $E_1(\text{LO})$ modes. These modes exhibit Raman frequency shifts in the

ZnO/ZnS and ZnO/ZnSe nanocomposites. It demonstrates stress and strain in the crystal structure. Moreover, the LO phonon peaks in the zinc blende (cubic phase) of ZnS and ZnSe indicate the existence of heterostructures form. The nanocomposite modifies the particle size of pristine ZnO. So, it means that structural modification of ZnO/ZnS and ZnO/ZnSe have been effectively synthesized using the solvothermal-microwave route. Therefore, the modified structure has the potential to be suitable for the optoelectronics field, such as solar cells.

References

- Raha S., Ahmaruzzaman M. ZnO nanostructured materials and their potential applications: progress, challenges and perspectives. *Nanoscale Advances*, 2022, vol. 8, no. 4, pp. 1868–1925. <https://doi.org/10.1039/d1na00880c>
- Theerthagiri J., Salla S., Senthil R.A., Nithyadharseni P., Madankumar A., Arunachalam P., Maiyalagan T., Kim H.-S. A review on ZnO nanostructured materials: energy, environmental and biological applications. *Nanotechnology*, 2019, vol. 30, no. 39, pp. 392001. <https://doi.org/10.1088/1361-6528/ab268a>
- Park T., Lee K.E., Kim N., Oh Y., Yoo J.-K., Um M.-K. Aspect ratio-controlled ZnO nanorods for highly sensitive wireless ultraviolet sensor applications. *Journal of Materials Chemistry C*, 2017, vol. 46, no. 5, pp. 12256–12263. <https://doi.org/10.1039/C7TC04671E>
- Chung D.S., Hall T.D., Cotella G., Lyu Q., Chun P., Aziz H. Significant lifetime enhancement in QLEDs by reducing interfacial charge accumulation via fluorine incorporation in the ZnO electron transport layer. *Nano-Micro Letters*, 2022, vol. 14, no. 1, pp. 212. <https://doi.org/10.1007/s40820-022-00970-x>
- Kumar M., Patra A. Highly efficient and Reusable ZnO microflower photocatalyst on stainless steel mesh under UV–Vis and natural sunlight. *Optical Materials*, 2020, vol. 107, pp. 110000. <https://doi.org/10.1016/j.optmat.2020.110000>
- Ali S., Saleem S., Salman M., Khan M. Synthesis, structural and optical properties of ZnS–ZnO nanocomposites. *Materials Chemistry and Physics*, 2020, vol. 248, pp. 122900. <https://doi.org/10.1016/j.matchemphys.2020.122900>
- Fang X., Zhai T., Gautam U.K., Li L., Wu L., Bando Y., Golberg D. ZnS nanostructures: From synthesis to applications. *Progress in Materials Science*, 2011, vol. 56, no. 2, pp. 175–287. <https://doi.org/10.1016/j.jpmatsci.2010.10.001>
- Kim J.S., Kim S.H., Lee H.S. Energy spacing and sub-band modulation of Cu doped ZnSe quantum dots. *Journal of Alloys and Compounds*, 2022, vol. 914, pp. 165372. <https://doi.org/10.1016/j.jallcom.2022.165372>
- Prabukanthan, P., Rajesh Kumar, T., Harichandran, G. Influence of various complexing agents on structural, morphological, optical and electrical properties of electrochemically deposited ZnSe thin films. *Journal of Materials Science: Materials in Electronics*, 2017, vol. 28, no. 19, pp. 14728–14737. <https://doi.org/10.1007/s10854-017-7341-4>
- Baranowska-Korczyc A., Kościński M., Coy E.L., Grześkowiak B.F., Jasiurkowska-Delaporte M. ZnS coating for enhanced environmental stability and improved properties of ZnO thin films. *RSC Advances*, 2018, vol. 8, no. 43, pp. 24411–24421. <https://doi.org/10.1039/c8ra02823k>
- Khan A.U., Tahir K., Albalawi K., Khalil M.Y., Almarhoon Z.M., Zaki M.E.A., Latif S., Hassan H.M.A., Refat M.S., Munshi A.M. Synthesis of ZnO and ZnS nanoparticles and their structural, optical, and photocatalytic properties synthesized via the wet chemical method. *Materials Chemistry and Physics*, 2022, vol. 291, pp. 126667. <https://doi.org/10.1016/j.matchemphys.2022.126667>
- Chen R., Cao J., Duan Y., Hui Y., Chuong T.T., Ou D., Han F., Cheng F., Huang X., Wu B., Zheng N. High-efficiency, hysteresis-less, UV-stable perovskite solar cells with cascade ZnO-ZnS electron transport layer. *Journal of the American Chemical Society*, 2019, vol. 141, no. 1, pp. 541–547. <https://doi.org/10.1021/jacs.8b11001>
- Cho S., Jang J.W., Lee J.S., Lee K.H. Porous ZnO-ZnSe nanocomposites for visible light photocatalysis. *Nanoscale*, 2012, vol. 4, no. 6, pp. 2066–2071. <https://doi.org/10.1039/c2nr11869f>

Литература

- Raha S., Ahmaruzzaman M. ZnO nanostructured materials and their potential applications: progress, challenges and perspectives // *Nanoscale Advances*. 2022. V. 8. N 4. P. 1868–1925. <https://doi.org/10.1039/d1na00880c>
- Theerthagiri J., Salla S., Senthil R.A., Nithyadharseni P., Madankumar A., Arunachalam P., Maiyalagan T., Kim H.-S. A review on ZnO nanostructured materials: energy, environmental and biological applications // *Nanotechnology*. 2019. V. 30. N 39. P. 392001. <https://doi.org/10.1088/1361-6528/ab268a>
- Park T., Lee K.E., Kim N., Oh Y., Yoo J.-K., Um M.-K. Aspect ratio-controlled ZnO nanorods for highly sensitive wireless ultraviolet sensor applications // *Journal of Materials Chemistry C*. 2017. V. 46. N 5. P. 12256–12263. <https://doi.org/10.1039/C7TC04671E>
- Chung D.S., Hall T.D., Cotella G., Lyu Q., Chun P., Aziz H. Significant lifetime enhancement in QLEDs by reducing interfacial charge accumulation via fluorine incorporation in the ZnO electron transport layer // *Nano-Micro Letters*. 2022. V. 14. N 1. P. 212. <https://doi.org/10.1007/s40820-022-00970-x>
- Kumar M., Patra A. Highly efficient and Reusable ZnO microflower photocatalyst on stainless steel mesh under UV–Vis and natural sunlight // *Optical Materials*. 2020. V. 107. P 110000. <https://doi.org/10.1016/j.optmat.2020.110000>
- Ali S., Saleem S., Salman M., Khan M. Synthesis, structural and optical properties of ZnS–ZnO nanocomposites // *Materials Chemistry and Physics*. 2020. V. 248. P. 122900, <https://doi.org/10.1016/j.matchemphys.2020.122900>
- Fang X., Zhai T., Gautam U.K., Li L., Wu L., Bando Y., Golberg D. ZnS nanostructures: From synthesis to applications // *Progress in Materials Science*. 2011. V. 56. N 2. P. 175–287. <https://doi.org/10.1016/j.jpmatsci.2010.10.001>
- Kim J.S., Kim S.H., Lee H.S. Energy spacing and sub-band modulation of Cu doped ZnSe quantum dots // *Journal of Alloys and Compounds*. 2022. V. 914. P. 165372. <https://doi.org/10.1016/j.jallcom.2022.165372>
- Prabukanthan, P., Rajesh Kumar T., Harichandran G. Influence of various complexing agents on structural, morphological, optical and electrical properties of electrochemically deposited ZnSe thin films // *Journal of Materials Science: Materials in Electronics*. 2017. V. 28. N 19. P. 14728–14737. <https://doi.org/10.1007/s10854-017-7341-4>
- Baranowska-Korczyc A., Kościński M., Coy E.L., Grześkowiak B.F., Jasiurkowska-Delaporte M. ZnS coating for enhanced environmental stability and improved properties of ZnO thin films // *RSC Advances*. 2018. V. 8. N 43. P. 24411–24421. <https://doi.org/10.1039/c8ra02823k>
- Khan A.U., Tahir K., Albalawi K., Khalil M.Y., Almarhoon Z.M., Zaki M.E.A., Latif S., Hassan H.M.A., Refat M.S., Munshi A.M. Synthesis of ZnO and ZnS nanoparticles and their structural, optical, and photocatalytic properties synthesized via the wet chemical method // *Materials Chemistry and Physics*. 2022. V. 291. P. 126667. <https://doi.org/10.1016/j.matchemphys.2022.126667>
- Chen R., Cao J., Duan Y., Hui Y., Chuong T.T., Ou D., Han F., Cheng F., Huang X., Wu B., Zheng N. High-efficiency, hysteresis-less, UV-stable perovskite solar cells with cascade ZnO-ZnS electron transport layer // *Journal of the American Chemical Society*. 2019. V. 141. N 1. P. 541–547. <https://doi.org/10.1021/jacs.8b11001>
- Cho S., Jang J.W., Lee J.S., Lee K.H. Porous ZnO-ZnSe nanocomposites for visible light photocatalysis // *Nanoscale*. 2012. V. 4. N 6. P. 2066–2071. <https://doi.org/10.1039/c2nr11869f>

14. Kamruzzaman M., Zapien J.A. Synthesis and characterization of ZnO/ZnSe NWs/PbS QDs solar cell. *Journal of Nanoparticle Research*, 2017, vol. 19, no. 4, pp. 125. <https://doi.org/10.1007/s11051-016-3729-y>
15. Krithika S., Balavijayalakshmi J. Synthesis of molybdenum disulfide doped zinc oxide nanocomposites by microwave assisted method. *Materials Research Express*, 2019, vol. 6, no. 10, pp. 105023. <https://doi.org/10.1088/2053-1591/ab3828>
16. Kumar V., Sharma H., Singh S.K., Kumar S., Vij A. Enhanced near-band edge emission in pulsed laser deposited ZnO/c-sapphire nanocrystalline thin films. *Applied Physics A: Materials Science and Processing*, 2019, vol. 125, no. 3, pp. 212. <https://doi.org/10.1007/s00339-019-2485-0>
17. Khan A. Raman spectroscopic study of the ZnO nanostructures. *Journal of the Pakistan Materials Society (JPMS)*, 2010, vol. 4, no. 1, pp. 5–9.
18. Ridwan J., Yunas J., Umar A.A., Mohd Raub A.A., Hamzah A.A., Kazmi J., Nandiyanto A.B.D., Pawinanto R.E., Hamidah I. Vertically aligned Cu-doped ZnO nanorods for photocatalytic activity enhancement. *International Journal of Electrochemical Science*, 2022, vol. 17, pp. 220813. <https://doi.org/10.20964/2022.08.10>
19. Abdelouhab Z.A., Djouadi D., Chelouche A., Touam T. Structural, morphological and Raman scattering studies of pure and Ce-doped ZnO nanostructures elaborated by hydrothermal route using nonorganic precursor. *Journal of Sol-Gel Science and Technology*, 2020, vol. 95, no. 1, pp. 136–145. <https://doi.org/10.1007/s10971-020-05293-0>
20. Sharma P., Bhati V.S., Kumar M., Sharma R., Mukhiya R., Awasthi K., Kumar M. Development of ZnO nanostructure film for pH sensing application. *Applied Physics A: Materials Science and Processing*, 2020, vol. 126, no. 4, pp. 284. <https://doi.org/10.1007/s00339-020-03466-w>
21. Bergman L., Chen X.B., Huso J., Morrison J.L., Hoeck H. Raman scattering of polar modes of ZnO crystallites. *Journal of Applied Physics*, 2005, vol. 98, no. 9, pp. 093507. <https://doi.org/10.1063/1.2126784>
22. Abdulrahman A.F., Ahmed S.M., Ahmed N.M., Almessiere M.A. Fabrication, characterization of ZnO nanorods on the flexible substrate (Kapton Tape) via chemical bath deposition for UV photodetector applications. *AIP Conference Proceedings*, 2017, vol. 1875, no. 1, pp. 020004. <https://doi.org/10.1063/1.4998358>
23. Cheng Y.C., Jin C.Q., Gao F., Wu X.L., Zhong W., Li S.H., Chu P.K. Raman scattering study of zinc blende and wurtzite ZnS. *Journal of Applied Physics*, 2009, vol. 106, no. 12, pp. 123505. <https://doi.org/10.1063/1.3270401>
24. Kao C.H., Su W.M., Li C.Y., Weng W.C., Cheng C.Y., Cheng C.-C., Lin Y.-S., Lin C.F., Chen H. Fabrication and characterization of ZnS/ZnO core shell nanostructures on silver wires. *AIP Advances*, 2018, vol. 8, no. 6, pp. 065106. <https://doi.org/10.1063/1.5027015>
25. Meng X., Li L., Li K., Zhou P., Zhang H., Jia J., Sun T. Desulfurization of fuels with sodium borohydride under the catalysis of nickel salt in polyethylene glycol. *Journal of Cleaner Production*, 2018, vol. 176, pp. 391–398. <https://doi.org/10.1016/j.jclepro.2017.12.152>
26. Zhou W., Liu R., Tang D., Zou B. The effect of dopant and optical micro-cavity on the photoluminescence of Mn-doped ZnSe nanobelts. *Nanoscale Research Letters*, 2013, vol. 8, no. 1, pp. 1–10. <https://doi.org/10.1186/1556-276X-8-314>
27. Yang X., Wang Q., Tao Y., Xu H. A modified method to prepare diselenides by the reaction of selenium with sodium borohydride. *Journal of Chemical Research — Part S*, 2002, pp. 160–161. <https://doi.org/10.3184/030823402103171726>
28. Shan C.X., Liu Z., Zhang X.T., Wong C.C., Hark S.K. Wurtzite ZnSe nanowires: Growth, photoluminescence, and single-wire Raman properties. *Nanotechnology*, 2006, vol. 17, no. 22, pp. 5561–5564. <https://doi.org/10.1088/0957-4484/17/22/006>
14. Kamruzzaman M., Zapien J.A. Synthesis and characterization of ZnO/ZnSe NWs/PbS QDs solar cell // *Journal of Nanoparticle Research*. 2017. V. 19. N 4. P. 125. <https://doi.org/10.1007/s11051-016-3729-y>
15. Krithika S., Balavijayalakshmi J. Synthesis of molybdenum disulfide doped zinc oxide nanocomposites by microwave assisted method // *Materials Research Express*. 2019. V. 6. N 10. P. 105023. <https://doi.org/10.1088/2053-1591/ab3828>
16. Kumar V., Sharma H., Singh S.K., Kumar S., Vij A. Enhanced near-band edge emission in pulsed laser deposited ZnO/c-sapphire nanocrystalline thin films // *Applied Physics A: Materials Science and Processing*. 2019. V. 125. N 3. P. 212. <https://doi.org/10.1007/s00339-019-2485-0>
17. Khan A. Raman spectroscopic study of the ZnO nanostructures // *Journal of the Pakistan Materials Society (JPMS)*. 2010. V. 4. N 1. P. 5–9.
18. Ridwan J., Yunas J., Umar A.A., Mohd Raub A.A., Hamzah A.A., Kazmi J., Nandiyanto A.B.D., Pawinanto R.E., Hamidah I. Vertically aligned Cu-doped ZnO nanorods for photocatalytic activity enhancement // *International Journal of Electrochemical Science*. 2022. V. 17. P. 220813. <https://doi.org/10.20964/2022.08.10>
19. Abdelouhab Z.A., Djouadi D., Chelouche A., Touam T. Structural, morphological and Raman scattering studies of pure and Ce-doped ZnO nanostructures elaborated by hydrothermal route using nonorganic precursor // *Journal of Sol-Gel Science and Technology*. 2020. V. 95. N 1. P. 136–145. <https://doi.org/10.1007/s10971-020-05293-0>
20. Sharma P., Bhati V.S., Kumar M., Sharma R., Mukhiya R., Awasthi K., Kumar M. Development of ZnO nanostructure film for pH sensing application // *Applied Physics A: Materials Science and Processing*. 2020. V. 126. N 4. P. 284. <https://doi.org/10.1007/s00339-020-03466-w>
21. Bergman L., Chen X.B., Huso J., Morrison J.L., Hoeck H. Raman scattering of polar modes of ZnO crystallites // *Journal of Applied Physics*. 2005. V. 98. N 9. P. 093507. <https://doi.org/10.1063/1.2126784>
22. Abdulrahman A.F., Ahmed S.M., Ahmed N.M., Almessiere M.A. Fabrication, characterization of ZnO nanorods on the flexible substrate (Kapton Tape) via chemical bath deposition for UV photodetector applications // *AIP Conference Proceedings*. 2017. V. 1875. N 1. P. 020004. <https://doi.org/10.1063/1.4998358>
23. Cheng Y.C., Jin C.Q., Gao F., Wu X.L., Zhong W., Li S.H., Chu P.K. Raman scattering study of zinc blende and wurtzite ZnS // *Journal of Applied Physics*. 2009. V. 106. N 12. P. 123505. <https://doi.org/10.1063/1.3270401>
24. Kao C.H., Su W.M., Li C.Y., Weng W.C., Cheng C.Y., Cheng C.-C., Lin Y.-S., Lin C.F., Chen H. Fabrication and characterization of ZnS/ZnO core shell nanostructures on silver wires // *AIP Advances*. 2018. V. 8. N 6. P. 065106. <https://doi.org/10.1063/1.5027015>
25. Meng X., Li L., Li K., Zhou P., Zhang H., Jia J., Sun T. Desulfurization of fuels with sodium borohydride under the catalysis of nickel salt in polyethylene glycol // *Journal of Cleaner Production*. 2018. V. 176. P. 391–398. <https://doi.org/10.1016/j.jclepro.2017.12.152>
26. Zhou W., Liu R., Tang D., Zou B. The effect of dopant and optical micro-cavity on the photoluminescence of Mn-doped ZnSe nanobelts // *Nanoscale Research Letters*. 2013. V. 8. N 1. P. 1–10. <https://doi.org/10.1186/1556-276X-8-314>
27. Yang X., Wang Q., Tao Y., Xu H. A modified method to prepare diselenides by the reaction of selenium with sodium borohydride // *Journal of Chemical Research — Part S*. 2002. P. 160–161. <https://doi.org/10.3184/030823402103171726>
28. Shan C.X., Liu Z., Zhang X.T., Wong C.C., Hark S.K. Wurtzite ZnSe nanowires: Growth, photoluminescence, and single-wire Raman properties // *Nanotechnology*. 2006. V. 17. N 22. P. 5561–5564. <https://doi.org/10.1088/0957-4484/17/22/006>

Authors

Yolanda Rati — Master Student, Institut Teknologi Bandung, Bandung, 40132, Indonesia, sc 57221219077, <https://orcid.org/0000-0003-0222-6014>, yolandarati@gmail.com
Ari Sulisty Rini — D.Sc., Senior Lecturer, Universitas Riau, Pekanbaru, 28293, Indonesia, sc 36059915000, <https://orcid.org/0000-0002-5435-2568>, ari.sulisty@lecturer.unri.ac.id

Авторы

Рати Иоланда — магистр, Бандунгский технологический институт, Бандунг, 40132, Индонезия, sc 57221219077, <https://orcid.org/0000-0003-0222-6014>, yolandarati@gmail.com
Рини Ари Сулисто — доктор наук, преподаватель, Университет Риау, Пеканбру, 28293, Индонезия, sc 36059915000, <https://orcid.org/0000-0002-5435-2568>, ari.sulisty@lecturer.unri.ac.id

Ali Umar Akrajas — D.Sc., Senior Lecturer, Universiti Kebangsaan Malaysia, Selangor, 43600, Malaysia,  9332520900, <https://orcid.org/0000-0001-8299-4827>, akrajas@ukm.edu.my
Miranti Agustin — Student, Universitas Riau, Pekanbaru, 28293, Indonesia,  57221219077, <https://orcid.org/0009-0007-1358-0496>, mirantiagustin17@gmail.com

Акраджас Али Умар — доктор наук, преподаватель, Национальный университет Малайзии, Селангор, 43600, Малайзия,  9332520900, <https://orcid.org/0000-0001-8299-4827>, akrajas@ukm.edu.my
Агустин Миранти — студент, Университет Риау, Пеканбару, 28293, Индонезия,  57221219077, <https://orcid.org/0009-0007-1358-0496>, mirantiagustin17@gmail.com

Received 02.09.2023

Approved after reviewing 06.11.2023

Accepted 27.11.2023

Статья поступила в редакцию 02.09.2023

Одобрена после рецензирования 06.11.2023

Принята к печати 27.11.2023



Работа доступна по лицензии
Creative Commons
«Attribution-NonCommercial»